

Purely optical macroscopic trap for alkaline-earth and similar atoms

O.N. Prudnikov,^{1,2} V. I. Yudin,^{1,2,3} R. Ya. Ilenkov,¹ and A. V. Taichenachev^{1,2}

¹*Institute of Laser Physics, Laser Physics Department, 630090, Novosibirsk, Russia*

²*Novosibirsk State University, Physics Department, 630090, Novosibirsk, Russia*

³*Novosibirsk State Technical University, Physics and Technology Department, 630073, Novosibirsk, Russia*

(*Electronic mail: oleg.nsu@gmail.com)

(Dated: 5 March 2026)

We consider a laser cooling and trapping of alkaline-earth and similar atoms in a bichromatic field resonant to a closed optical transition $^1S_0 \rightarrow ^1P_1$ or $^1S_0 \rightarrow ^3P_1$. It is shown that new kinetic effects emerge compared to monochromatic fields, enabling the formation of a deep macroscopic trap capable of capturing and cooling neutral atoms to sub-Doppler temperatures. Such a purely optical macroscopic trap can serve as an alternative to the well-known magneto-optical trap and can be used in applications requiring minimization of the magnetic field in the cold atom cloud region. The obtained results are of interest for the new generation of quantum sensors and optical frequency standards.

Keywords: Recoil effects, laser cooling, macroscopic optical trap

I. INTRODUCTION

As is well known¹, efficient laser cooling of atoms is possible due to the action of Doppler and sub-Doppler mechanisms leading to dissipation of the atom kinetic energy in the field of counter-propagating waves resonant to the optical transition. However, in most cases, experiments with cold atoms requires not only cooling to low temperatures, but also reliable trapping. This has stimulated work on searching for configurations of light fields capable of forming deep dissipative traps for cooling and holding of atoms. The most successful solution to this problem is the magneto-optical trap (MOT), proposed and experimentally realized in the late 1980s². The unique combination of an inhomogeneous magnetic field and counter-propagating light waves forms a deep magneto-optical potential, allowing for cooling and trapping of atoms.

On the other hand, the creation of modern high-precision quantum devices based on cold atoms (such as atomic clocks, quantum logic gates, quantum memory, atomic interferometers, gravimeters, gyroscopes, etc.) imposes new requirements that may pose significant challenges when using a standard magneto-optical trap. One such requirement is the precise control of the magnetic field in the region where cold atoms are interrogated as a quantum object. Therefore, the search for new mechanisms for cooling and trapping atoms without use of magnetic field is particularly relevant, especially in compact devices. For example in Ref.³, we proposed the idea of deep dissipative potential of macroscopic scale in bichromatic field for cooling and trapping of Li atoms, which have a specific structure of energy levels. The components of the bichromatic field are resonant to different optical transitions, allowing the formation of purely optical macroscopic traps with relatively low field intensities comparable to those used in MOTs. The formed deep dissipative trap is determined by a combination of two effects. First, the dipole force rectification in a bichromatic field, predicted in^{4,5} and used for effective slowing of atomic beams⁶⁻⁸. Second, dissipative mechanisms of laser cooling in a bichromatic field^{9,10}. The spa-

tial beating of optical shifts of atomic levels in a bichromatic field forms a macroscopic potential with a period $\Lambda = \pi/|\Delta\mathbf{k}|$, where $\Delta\mathbf{k} = \mathbf{k}_2 - \mathbf{k}_1$ is the difference in the wave vectors of the frequency components of the bichromatic field. When the frequency difference is chosen in the range of 5 – 30 GHz, the macroscopic period of the optical trap has a centimeter scale, enabling sub-millimeter sizes of the trapped atoms cloud. For demonstration of this effect, in³, transitions between fine or hyperfine structure levels of lithium atoms were considered. However, not for all elements the optical transitions with the above frequency differences can be found.

In the present work, we are developing the idea of purely optical macroscopic dissipative trap for the atoms in which the energy levels structure does not contain transitions with frequency differences in the range of 5 – 30 GHz. For these atoms to create a deep macroscopic potential, we consider a bichromatic field with the required frequency difference interacting with the same atomic transition. The case under consideration does not require a specific structure of fine or hyperfine levels (as in³) and can be realized for most alkaline-earth-like atoms (e.g., Ca, Sr, Ba, Hg, Mg, Yb, see Table I), which have a dipole-allowed closed optical transition. These elements are of particular interest for optical frequency standards¹¹⁻¹⁶, quantum memory¹⁷, and atomic interferometers¹⁸⁻²¹. We demonstrate that a deep dissipative macroscopic trapping potential can be formed. Moreover, sub-Doppler temperature can be reached in it for odd isotopes.

II. KINETICS OF ATOMS IN A BICHROMATIC FIELD

Let us consider the interaction of atoms with a bichromatic laser field having frequency components ω_1 and ω_2

$$\mathbf{E}(\mathbf{r}, t) = \text{Re} \left\{ \sum_{\alpha=1,2} \mathbf{E}_{\alpha}(\mathbf{r}) e^{-i\omega_{\alpha}t} \right\}, \quad (1)$$

which are resonant to an optical transition with frequency ω_0 . The optical transitions used for laser cooling of alkaline-earth-like atoms have the electron configuration $J_g = 0 \rightarrow J_e = 1$

element	nuclear spin	laser cooling transition	$\gamma/2\pi$ (MHz)	I_S (mW/cm ²)	λ (nm)	ϵ_R
²⁵ Mg, ²⁴ Mg	5/2, 0	$3^1S_0 \rightarrow 3^1P_1$	79	439	285.3	$1.3 \cdot 10^{-3}$
⁴⁰ Ca	0	$4^1S_0 \rightarrow 4^1P_1$	35.7	61.9	422.6	$7.8 \cdot 10^{-4}$
⁸⁷ Sr, ⁸⁸ Sr	9/2, 0	$5^1S_0 \rightarrow 5^1P_1$ $5^1S_0 \rightarrow 5^3P_1$	32 $7.5 \cdot 10^{-3}$	42.7 $2.8 \cdot 10^{-3}$	461 689	$3.4 \cdot 10^{-4}$ 0.64
¹³⁵ Ba, ¹³⁸ Ba	3/2, 0	$6^1S_0 \rightarrow 6^1P_1$ $6^1S_0 \rightarrow 6^3P_1$	18.9 0.048	14.6 $12.5 \cdot 10^{-3}$	553.7 791.3	$2.5 \cdot 10^{-4}$ 0.048
¹⁷¹ Yb, ¹⁷⁴ Yb	1/2, 0	$6^1S_0 \rightarrow 6^1P_1$ $6^1S_0 \rightarrow 6^3P_1$	29 0.18	59 0.14	399 555.8	$2.5 \cdot 10^{-4}$ 0.02
¹⁹⁹ Hg, ²⁰⁰ Hg	1/2, 0	$6^1S_0 \rightarrow 6^1P_1$ $6^1S_0 \rightarrow 6^3P_1$	120 1.3	2480 10.6	185 253.7	$2.4 \cdot 10^{-4}$ 0.012

TABLE I. Optical transitions of alkaline-earth-like atoms for laser cooling, their parameters (data from^{13,18,22–25}): wavelength λ , saturation intensity ($I_S = 2\pi^2\hbar c\gamma/\lambda^3$) and recoil parameter $\epsilon_R = \hbar k^2/(2M\gamma)$ is equal to the ratio of the recoil energy to the natural linewidth (M is the mass of the atom).

(see Table I), where J_g and J_e are the electron angular momenta of the ground (g) and excited (e) states, respectively. For odd isotopes with non-zero nuclear spin I (see Table I), a set of excited states emerges with total angular momentum F_{e_n} , where $|J_e - I| \leq F_{e_n} \leq |J_e + I|$, while the ground state has angular momentum $F_g = I$. Such level structure exists for the dipole transition $^1S_0 \rightarrow ^1P_1$ and intercombination dipole transition $^1S_0 \rightarrow ^3P_1$. It should be noted that the natural linewidth of the intercombination transition increases with the atomic number, which allows it to be used for laser cooling of heavy elements^{26–28}.

The Hamiltonian of an atom interacting with a laser field has the form

$$\hat{H} = \frac{\hat{p}^2}{2M} + \hat{H}_0 + \hat{W}(t), \quad (2)$$

where the first term is the kinetic energy operator, the second is the Hamiltonian of the atom in the rest frame, and the last term is atom-light interaction part. The Hamiltonian \hat{H}_0 can be written in a form $\hat{H}_0 = \hat{H}_0^{ee} + \hat{H}_0^{gg}$, where the blocks for the ground and excited states are defined through the projection operators \hat{P}^{e_n} and \hat{P}^g as follows

$$\begin{aligned} \hat{H}_0^{ee} &= \sum_n \mathcal{E}_{e_n} \hat{P}^{e_n}, \quad \hat{P}^{e_n} = \sum_{M_{e_n}} |F_{e_n}, M_{e_n}\rangle \langle F_{e_n}, M_{e_n}| \\ \hat{H}_0^{gg} &= \mathcal{E}_g \hat{P}^g, \quad \hat{P}^g = \sum_{M_g} |F_g, M_g\rangle \langle F_g, M_g|. \end{aligned} \quad (3)$$

Here \mathcal{E}_{e_n} is the energy of the n -th excited state, \mathcal{E}_g is the energy of the ground state, $|F_{e_n}, M_{e_n}\rangle$ and $|F_g, M_g\rangle$ describe the wave functions of the Zeeman sublevels in the excited and ground states, where M_{e_n} and M_g are magnetic quantum numbers ($-F_{e_n} \leq M_{e_n} \leq F_{e_n}$, $-F_g \leq M_g \leq F_g$). The atom-light

interaction in the electric dipole approximation can be written as

$$\begin{aligned} \hat{W}(\mathbf{r}, t) &= \hbar \sum_{\alpha=1,2} \hat{V}_\alpha(\mathbf{r}) e^{-i\omega_\alpha t} + h.c., \\ \hat{V}_\alpha(\mathbf{r}) &= -(\mathbf{E}_\alpha(\mathbf{r}) \cdot \hat{\mathbf{D}}) \bar{d}/2\hbar, \end{aligned} \quad (4)$$

where \bar{d} is the reduced matrix element of the dipole transition for considered electron transition $J_g = 0 \rightarrow J_e = 1$, $\hat{\mathbf{D}}$ is the normalized (dimensionless) operator of the dipole moment of the atom, whose components \hat{D}_s ($s = 0, \pm 1$) in the cyclic basis $\{\mathbf{e}_\pm = \mp(\mathbf{e}_x \pm i\mathbf{e}_y)/\sqrt{2}, \mathbf{e}_0 = \mathbf{e}_z\}$ are expressed through the Clebsch-Gordan coefficients

$$\hat{D}_s = \sum_{F_{e_n}, M_{e_n}, M_g} |F_{e_n}, M_{e_n}\rangle C_{F_g, M_g; 1, s}^{F_{e_n}, M_{e_n}} \langle F_g, M_g|. \quad (5)$$

The quantum kinetic equation describing the evolution of the atomic density matrix in the field (1) with full consideration of recoil effects has the following form in coordinate representation

$$\begin{aligned} \frac{\partial}{\partial t} \hat{\rho}(\mathbf{r}_1, \mathbf{r}_2) &= \\ &- \frac{i}{\hbar} [\hat{H}(\mathbf{r}_1) \hat{\rho}(\mathbf{r}_1, \mathbf{r}_2) - \hat{\rho}(\mathbf{r}_1, \mathbf{r}_2) \hat{H}(\mathbf{r}_2)] - \hat{\Gamma}\{\hat{\rho}(\mathbf{r}_1, \mathbf{r}_2)\}. \end{aligned} \quad (6)$$

The last term describes the non-Hamiltonian evolution of the quantum system as a result of spontaneous relaxation taking into account recoil effects (see, for example,²⁹):

$$\begin{aligned} \hat{\Gamma}\{\hat{\rho}\} &= \frac{\gamma}{2} (\hat{P}^e \hat{\rho} + \hat{\rho} \hat{P}^e) - \hat{\gamma}\{\hat{\rho}\} \\ \hat{\gamma}\{\hat{\rho}\} &= \gamma \frac{3}{2} \left\langle \sum_{\xi=1,2} (\hat{\mathbf{D}} \cdot \mathbf{e}_\xi(\mathbf{k}))^\dagger e^{-i\mathbf{k}\hat{\mathbf{r}}_1} \hat{\rho} e^{i\mathbf{k}\hat{\mathbf{r}}_2} (\hat{\mathbf{D}} \cdot \mathbf{e}_\xi(\mathbf{k})) \right\rangle. \end{aligned} \quad (7)$$

Here $\hat{P}^e = \sum_n \hat{P}^{e_n}$ is the full projector onto all excited states, and γ is the natural linewidth. The operator $\hat{\gamma}\{\hat{\rho}\}$ describes the arrival to the ground state from excited states due to spontaneous emission, where $\langle \dots \rangle$ means averaging over the emission directions of spontaneous photons with momentum $\hbar\mathbf{k}$ and two mutually orthogonal polarizations $\mathbf{e}_\xi(\mathbf{k})$.

As noted in the introduction, to create a deep dissipative po-

tential with a centimeter scale, it is necessary to use the fields with a frequency difference of $|\omega_1 - \omega_2| \sim 5 - 30$ GHz. Such a difference in frequencies allows us to neglect the rapidly oscillating contributions $\exp(\pm i(\omega_1 - \omega_2)t)$ in equation (6). As a result, in the rotating-wave approximation, we obtain the following system of equations for the matrix blocks $\hat{\rho}(\mathbf{r}_1, \mathbf{r}_2)$

$$\begin{aligned}
\frac{d}{dt}\hat{\rho}^{ee}(\mathbf{r}_1, \mathbf{r}_2) &= -\gamma\hat{\rho}^{ee}(\mathbf{r}_1, \mathbf{r}_2) - \frac{i}{\hbar}\left[\hat{H}_0^{ee}\hat{\rho}^{ee}(\mathbf{r}_1, \mathbf{r}_2) - \hat{\rho}^{ee}(\mathbf{r}_1, \mathbf{r}_2)\hat{H}_0^{ee}\right] \\
&\quad - i\sum_{\alpha=1,2}\left(\hat{V}_\alpha(\mathbf{r}_1)\hat{\rho}_\alpha^{se}(\mathbf{r}_1, \mathbf{r}_2) - \hat{\rho}_\alpha^{se}(\mathbf{r}_1, \mathbf{r}_2)\hat{V}_\alpha^\dagger(\mathbf{r}_2)\right) \\
\frac{d}{dt}\hat{\rho}^{gg}(\mathbf{r}_1, \mathbf{r}_2) &= \hat{\gamma}\{\hat{\rho}^{ee}(\mathbf{r}_1, \mathbf{r}_2)\} - \frac{i}{\hbar}\left[\hat{H}_0^{gg}\hat{\rho}^{gg}(\mathbf{r}_1, \mathbf{r}_2) - \hat{\rho}^{gg}(\mathbf{r}_1, \mathbf{r}_2)\hat{H}_0^{gg}\right] \\
&\quad - i\sum_{\alpha=1,2}\left(\hat{V}_\alpha^\dagger(\mathbf{r}_1)\hat{\rho}_\alpha^{eg}(\mathbf{r}_1, \mathbf{r}_2) - \hat{\rho}_\alpha^{eg}(\mathbf{r}_1, \mathbf{r}_2)\hat{V}_\alpha(\mathbf{r}_2)\right) \\
\frac{d}{dt}\hat{\rho}_\alpha^{eg}(\mathbf{r}_1, \mathbf{r}_2) &= -\left(\frac{\gamma}{2} - i\omega_\alpha\right)\hat{\rho}_\alpha^{eg}(\mathbf{r}_1, \mathbf{r}_2) - \frac{i}{\hbar}\left[\hat{H}_0^{ee}\hat{\rho}_\alpha^{eg}(\mathbf{r}_1, \mathbf{r}_2) - \hat{\rho}_\alpha^{eg}(\mathbf{r}_1, \mathbf{r}_2)\hat{H}_0^{gg}\right] \\
&\quad - i\left(\hat{V}_\alpha(\mathbf{r}_1)\hat{\rho}^{gg}(\mathbf{r}_1, \mathbf{r}_2) - \hat{\rho}^{ee}(\mathbf{r}_1, \mathbf{r}_2)\hat{V}_\alpha(\mathbf{r}_2)\right), \quad \alpha = 1, 2 \\
\frac{d}{dt}\hat{\rho}_\alpha^{se}(\mathbf{r}_1, \mathbf{r}_2) &= -\left(\frac{\gamma}{2} + i\omega_\alpha\right)\hat{\rho}_\alpha^{se}(\mathbf{r}_1, \mathbf{r}_2) - \frac{i}{\hbar}\left[\hat{H}_0^{gg}\hat{\rho}_\alpha^{se}(\mathbf{r}_1, \mathbf{r}_2) - \hat{\rho}_\alpha^{se}(\mathbf{r}_1, \mathbf{r}_2)\hat{H}_0^{ee}\right] \\
&\quad - i\left(\hat{V}_\alpha^\dagger(\mathbf{r}_1)\hat{\rho}^{ee}(\mathbf{r}_1, \mathbf{r}_2) - \hat{\rho}^{gg}(\mathbf{r}_1, \mathbf{r}_2)\hat{V}_\alpha^\dagger(\mathbf{r}_2)\right), \quad \alpha = 1, 2,
\end{aligned} \tag{8}$$

where matrix blocks are defined by the following

$$\begin{aligned}
\hat{\rho}^{gg} &= \hat{P}^g\hat{\rho}\hat{P}^g, \quad \hat{\rho}^{ee} = \hat{P}^e\hat{\rho}\hat{P}^e, \\
\hat{\rho}^{eg} &= \hat{P}^e\hat{\rho}\hat{P}^g = \hat{\rho}_1^{eg}e^{-i\omega_1 t} + \hat{\rho}_2^{eg}e^{-i\omega_2 t}, \quad \hat{\rho}^{se} = (\hat{\rho}^{eg})^\dagger,
\end{aligned} \tag{9}$$

Here $\hat{\rho}^{gg}$ and $\hat{\rho}^{ee}$ describe atoms in the ground and excited states, $\hat{\rho}_\alpha^{eg}$, $\hat{\rho}_\alpha^{se}$ ($\alpha = 1, 2$) are the slow amplitudes of the off-diagonal elements of the density matrix. For brevity in (8), we use

$$\frac{d}{dt} = \frac{\partial}{\partial t} - i\frac{\hbar}{2M}\frac{\partial^2}{\partial \mathbf{r}_1^2} + i\frac{\hbar}{2M}\frac{\partial^2}{\partial \mathbf{r}_2^2}. \tag{10}$$

As well known³⁰⁻³², the equation for the atomic density matrix in the Wigner representation $\hat{\rho}(\mathbf{r}, \mathbf{p})$ by means of expansion in terms of the recoil parameter $\hbar k/\Delta p \ll 1$ (Δp is the width of the momentum distribution of the ensemble of atoms) can be reduced to the Fokker-Planck equation for the distribution function in the phase space $\mathcal{F}(\mathbf{r}, \mathbf{p}) = \text{Tr}\{\hat{\rho}(\mathbf{r}, \mathbf{p})\}$

$$\begin{aligned}
\left(\frac{\partial}{\partial t} + \frac{\mathbf{p}}{M} \cdot \frac{\partial}{\partial \mathbf{r}}\right)\mathcal{F}(\mathbf{r}, \mathbf{p}) &= -\sum_j \frac{\partial}{\partial p_j} F_j(\mathbf{r}, \mathbf{p})\mathcal{F}(\mathbf{r}, \mathbf{p}) \\
&\quad + \sum_{jj'} \frac{\partial}{\partial p_j} \frac{\partial}{\partial p_{j'}} D_{jj'}(\mathbf{r}, \mathbf{p})\mathcal{F}(\mathbf{r}, \mathbf{p}),
\end{aligned} \tag{11}$$

with coefficients corresponding to the force $\mathbf{F}(\mathbf{r}, \mathbf{p})$ acting on the atom and the diffusion tensor $D_{jj'}(\mathbf{r}, \mathbf{p})$. Note that the results obtained within the semiclassical approach based on the Fokker-Planck equation (11) are well agreed with the results

of direct quantum simulation in the case of small recoil parameter $\epsilon_R = \hbar k^2/(2M\gamma) \ll 1$ ³³⁻³⁵. Since the condition $\epsilon_R \ll 1$ is satisfied quite well for the elements under consideration (see table I), below we will use semiclassical approximation.

To obtain expressions for the force and diffusion, we use the method proposed in^{36,37}. The essence of the method is that the expansion of the quantum kinetic equation on recoil parameter $\hbar k/\Delta p \ll 1$ in coordinate representation (6), rewritten in variables

$$\mathbf{q} = \mathbf{r}_1 - \mathbf{r}_2, \quad \mathbf{r} = (\mathbf{r}_1 + \mathbf{r}_2)/2, \tag{12}$$

is equivalent to expansion in powers of $-ikq_j$, where q_j are the Cartesian components of the vector \mathbf{q} . This expansion can be written in the general operator form

$$\begin{aligned}
\left(\frac{\partial}{\partial t} - i\frac{\hbar}{M}\frac{\partial}{\partial \mathbf{q}} \cdot \frac{\partial}{\partial \mathbf{r}}\right)\hat{\rho}(\mathbf{r}, \mathbf{q}) &= \mathcal{L}^{(0)}\{\hat{\rho}\} \\
&\quad - \sum_j ikq_j \mathcal{L}_j^{(1)}\{\hat{\rho}\} + \sum_{jj'} (-ik)^2 q_j q_{j'} \mathcal{L}_{jj'}^{(2)}\{\hat{\rho}\} \dots,
\end{aligned} \tag{13}$$

where the explicit expressions of the operators $\mathcal{L}^{(k)}$ are given in Appendix A. Note that the transition from coordinate representation (12) to Wigner is defined by Fourier transformation

$$\hat{\rho}(\mathbf{r}, \mathbf{p}) = \int \hat{\rho}(\mathbf{r}, \mathbf{q}) e^{-i\mathbf{p}\mathbf{q}/\hbar} d\mathbf{q} / (2\pi\hbar)^3. \tag{14}$$

Following the proposed methods^{36,37}, the equation (13) within the semiclassical approach can be reduced to the Fokker-Planck equation (11) for the distribution function in the phase

space $\mathcal{F}(\mathbf{r}, \mathbf{p})$. In this case, the expression for the force $\mathbf{F}(\mathbf{r}, \mathbf{p})$ is determined by the first-order terms in the expansion (13). The Cartesian component of the force F_j acting on the atom with the velocity $\mathbf{v} = \mathbf{p}/M$ has the form:

$$F_j(\mathbf{r}, \mathbf{p}) = -\text{Tr}\left\{\mathcal{L}_j^{(1)}\{\hat{\sigma}(\mathbf{r}, \mathbf{p})\}\right\}, \quad (15)$$

where $\hat{\sigma}(\mathbf{r}, \mathbf{p})$ is a stationary solution of the optical Bloch equation

$$\frac{\mathbf{p}}{M} \cdot \frac{\partial}{\partial \mathbf{r}} \hat{\sigma} = \mathcal{L}^{(0)}\{\hat{\sigma}\}, \quad \text{Tr}\{\hat{\sigma}\} = 1. \quad (16)$$

The diffusion coefficient is split into the sum of two contributions

$$D_{jj'} = D_{jj'}^{(sp)} + D_{jj'}^{(ind)}. \quad (17)$$

The first term in it is the spontaneous diffusion tensor, determined by the fluctuation of the atomic momentum during spontaneous emission of photons

$$D_{jj'}^{(sp)}(\mathbf{r}, \mathbf{p}) = \hbar^2 k^2 \text{Tr}\left\{\mathcal{L}_{jj'}^{(2)}\{\hat{\sigma}\}\right\} = \frac{\hbar^2 k^2 \gamma}{5} \text{Tr}\left\{\left(\delta_{jj'} \hat{P}^e - \frac{1}{4}(\hat{D}_j \hat{D}_{j'}^\dagger + \hat{D}_{j'} \hat{D}_j^\dagger)\right) \hat{\sigma}(\mathbf{r}, \mathbf{p})\right\}, \quad (18)$$

where $\delta_{jj'}$ is the Kronecker symbol. The second term in (17) is the tensor of induced diffusion, is determined by the fluctuation of the atomic momentum in the processes of induced absorption/emission of field photons

$$D_{jj'}^{(ind)} = \hbar^2 k^2 \text{Tr}\left\{\mathcal{L}_j^{(1)}\{\hat{\eta}_{j'}\}\right\}, \quad (19)$$

where the matrix $\hat{\eta}_j(\mathbf{r}, \mathbf{p})$ satisfies the equation

$$\begin{aligned} \frac{\mathbf{p}}{M} \cdot \frac{\partial}{\partial \mathbf{r}} \hat{\eta}_j &= \mathcal{L}^{(0)}\{\hat{\eta}_j\} + \mathcal{L}_j^{(1)}\{\hat{\sigma}\} - \hat{\sigma} \text{Tr}\left\{\mathcal{L}_j^{(1)}\{\hat{\sigma}\}\right\} \\ \text{Tr}\{\hat{\eta}_j\} &= 0, \end{aligned} \quad (20)$$

which is equivalent to the approach developed in^{31,32}.

Note that for the model of a two-level atom^{9,10} we obtained analytical expressions for the optical potential, friction coefficients (linear in velocity correction to the force) and the diffusion tensor in the limit of low velocities. However, to analyze the possibility of sub-Doppler laser cooling it is necessary to get expressions for the force and diffusion beyond the low-velocity approximation $kv \ll \gamma$. The equations (15)-(20) allow us to obtain the required expressions for the force and diffusion tensors in a bichromatic field and to analyze sub-Doppler cooling taking into account the real hyperfine and Zeeman structure of atomic levels.

III. NUMERICAL CALCULATIONS OF LASER COOLING AND TRAPPING OF ATOMS

As a specific example, in this section we consider the ¹⁷¹Yb atom, whose levels are degenerate in the projection of the angular momentum (Fig. 1), which is a necessary condition for

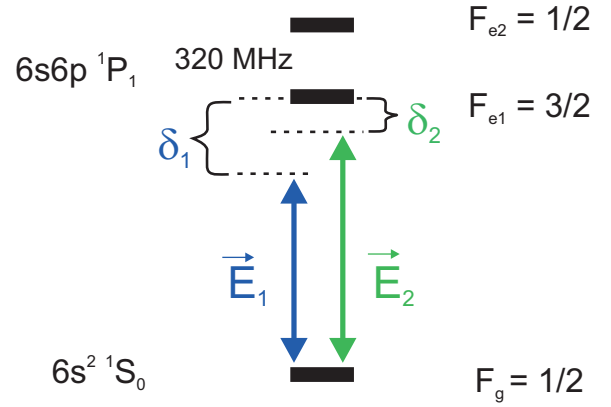


FIG. 1. The scheme of energy levels of ytterbium-171 for laser cooling and trapping in a bichromatic field. Solid arrows represents transitions induced by components of the bichromatic field \mathbf{E}_1 and \mathbf{E}_2 .

sub-Doppler cooling³⁸. In this case, we consider the double *lin* \perp *lin* configuration of the light field proposed by us³ to form a macroscopic potential. In this case, both fields \mathbf{E}_1 and \mathbf{E}_2 in the expression (1) are formed by counterpropagating waves with orthogonal linear polarizations (Fig. 2)

$$\mathbf{E}_\alpha(z) = E_{0\alpha} \left(\mathbf{e}_x e^{ik_\alpha z} + \mathbf{e}_y e^{-ik_\alpha z} \right), \quad \alpha = 1, 2, \quad (21)$$

where $k_\alpha = \omega_\alpha/c$ are the wave vectors (c is the speed of light), and $E_{0\alpha}$ are the amplitudes of the corresponding running wave. We choose δ_1 and δ_2 as the detunings of the frequency components ω_1 and ω_2 from the resonance with the optical transition $F_g = 1/2 \rightarrow F_e = 3/2$ (Fig. 1). In this case, both fields have close wave vectors $k_2 \simeq k_1 = k$, $\Delta k = k_2 - k_1 \ll k$, and their relative phase $\Delta\phi = \Delta k z = (\delta_2 - \delta_1)z/c$ is a slow function of the coordinate, which determines the macroscopic period of the bichromatic potential^{3,9,10}

$$\Lambda = \frac{\pi c}{|\omega_2 - \omega_1|} = \frac{\pi c}{|\delta_2 - \delta_1|}. \quad (22)$$

To form dissipative mechanisms of laser cooling, we choose detuning δ_2 is close to resonance with the transition $F_g = 1/2 \rightarrow F_e = 3/2$. Then, as follows from (22), the value $|\delta_1|$ must be chosen in the range 5 – 30 GHz to form a centimeter-scale macroscopic potential.

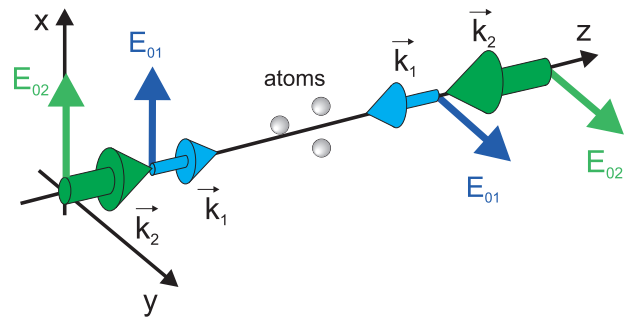


FIG. 2. Double *lin* \perp *lin* bichromatic field configuration.

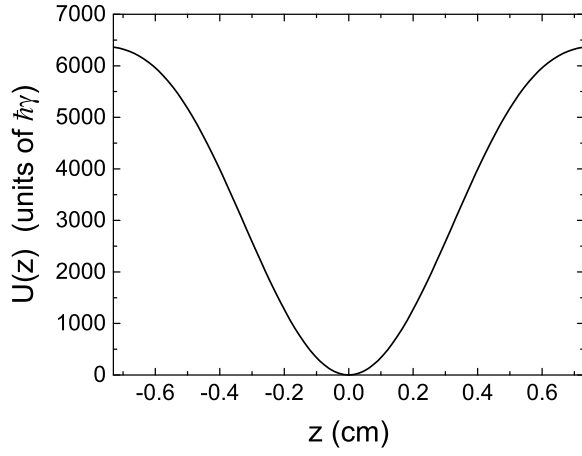


FIG. 3. Macroscopic optical potential $U(z)$ in units of $\hbar\gamma$ in a bichromatic field. Field detunings $\delta_1 = -346\gamma$ ($\simeq 10\text{GHz}$), and $\delta_2 = -3\gamma$. Intensities of the waves of the frequency components $I_1 \simeq 57\text{ W/cm}^2$ ($\Omega_{01} \simeq 22\gamma$), and $I_2 \simeq 0.4\text{ W/cm}^2$ ($\Omega_{02} \simeq 1.9\gamma$).

Fig. 3 shows a typical dependence of the macroscopic optical potential formed for ^{171}Yb atoms in double $\text{lin}\perp\text{lin}$ configuration (21). For example, for detunings $\delta_1 = -346\gamma$ ($\simeq 10\text{GHz}$), $\delta_2 = -3\gamma$, the period of macroscopic potential is $\Lambda = 1.2\text{ cm}$. In this case, for the intensities of the running waves $I_1 \simeq 57\text{ W/cm}^2$ ($\Omega_{01} \simeq 22\gamma$) and $I_2 \simeq 0.4\text{ W/cm}^2$ ($\Omega_{02} \simeq 1.9\gamma$) the depth of the optical potential reaches $\Delta U_{\text{opt}} \simeq 6400\hbar\gamma$, (or $\sim 8.8\text{K}$ in temperature units), which is comparable with the depth of magneto-optical traps and is quite sufficient for capturing, cooling and holding of atoms.

The dependences of the force on the velocity at the center and at the slope of the optical potential are shown in Fig. 4. As can be seen, in the low-velocity region the force has a typical dependence of sub-Doppler mechanisms of laser cooling³⁸. Also, for velocities $v = \pm|\delta_2|/k$ there are maxima caused by the resonance of atoms of a given velocity group with counter

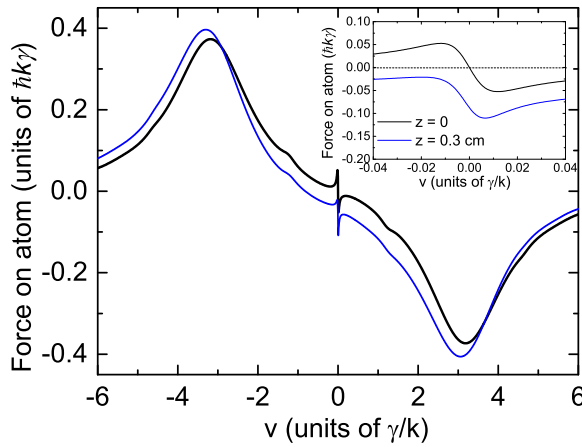


FIG. 4. Force on an atom moving with velocity v in a bichromatic field in the region of the global minimum of the optical potential $z = 0$ (black line) and on the slope of the optical potential $z = 0.3\text{ cm}$ (blue line). The field parameters correspond to Fig.3.

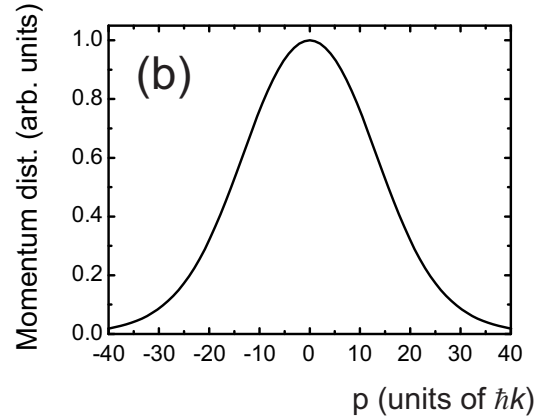
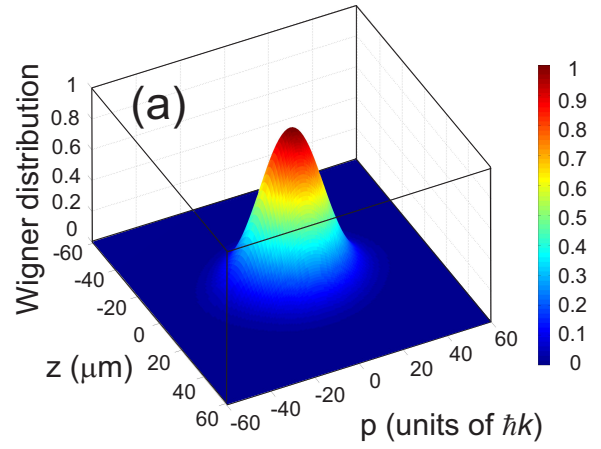


FIG. 5. The Wigner function of (a) the atomic phase distribution $\mathcal{F}(z, p)$ and (b) the momentum distribution of cold atoms in the macroscopic potential of the bichromatic field of double $\text{lin}\perp\text{lin}$ configuration. The field parameters correspond to Fig.3.

traveling waves of \mathbf{E}_2 field as a result of the Doppler effect. Note that the presence of another hyperfine component $F_{e_2} = 1/2$ leads to additional resonances in the dependence of the force on the velocity of those spaced by $\delta v = \Delta_{hf}/k \simeq 11\gamma/k$ (outside the region of Fig. 4). When shifting from the center of the optical trap, the effect of rectification of the dipole force in a wide range of velocities is clearly seen (see the blue line in Fig.4).

The temperature and size of trapped atoms in such a potential can be obtained from steady-state solution of the Fokker-Planck equation (11). For the parameters of Fig. 3, the laser cooling temperature reaches sub-Doppler values of $T \simeq 0.1\hbar\gamma/k_B \sim 130\mu\text{K}$ (see Fig. 5), and the size of the atomic cloud is $\sim 28\mu\text{m}$. Note that the Doppler temperature achievable in the MOT at the transition under consideration $F_g = 1/2 \rightarrow F_e = 3/2$ is of the order of $T_D \simeq 0.5\hbar\gamma/k_B \sim 700\mu\text{K}$, because of sub-Doppler cooling mechanisms in standard MOT formed by field of the $\sigma_+ - \sigma_-$ configuration are absent for this transition³⁸.

One of the important characteristics of a dissipative trap is the ability to capture atoms directly from the hot vapor. The

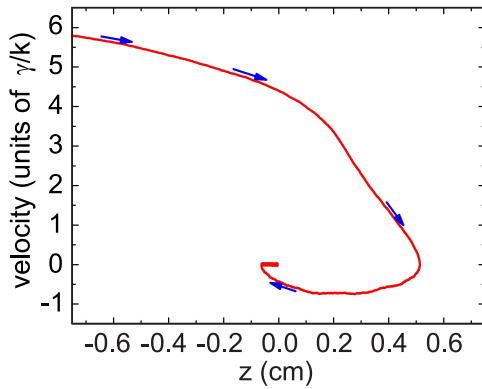


FIG. 6. The phase-space trajectory of an atom entering to the macroscopic optical trap formed by double $lin \perp lin$ configuration of bichromatic field with parameters of Fig.3. The initial velocity of atoms on the trap boundary $v_c = 5.8\gamma/k \simeq 67$ m/s. The blue arrows indicate the direction of the trajectory evolution.

number of captured atoms can be estimated from the relation presented in^{39,40}

$$N_c = \frac{L^2}{\sigma_c} \left(\frac{v_c}{u} \right)^4, \quad (23)$$

where v_c is the velocity at which atoms are captured in the trap, $u = (2k_B T/M)^{1/2}$ is the most probable velocity of atoms in a vapor (170 m/s for ytterbium atoms at $T = 300$ K), L is the size of the trap, and σ_c is the cross-section for an atom to eject an atom from the trap. Therefore, the number of trapped atoms can be increased via the use of field configurations that maximize v_c , or by using additional Zeeman slower of the atomic beam to effectively reduce u . The Fig. 6 shows the trajectory of an atom in the phase space (z, v) entering into the trap. The trajectory is calculated based on the Langevin equations (see, for example,^{41,42}) describing the atom trajectory under the light force and associated stochastic diffusion. The velocity at which atoms are able to be captured into the trap is $v_c \simeq 5.8\gamma/k \simeq 67$ m/s for the parameters of Fig. 3. This leads to a theoretical estimate of the number of captured atoms $N_c \simeq 4 \times 10^{11}$, which is comparable to the number of atoms captured in a magneto-optical trap.

IV. MULTIDIMENSIONAL OPTICAL LATTICES OF MACROSCOPIC SCALE

2D and 3D configurations of macroscopic optical lattices can be formed in space by superimposing several traveling bichromatic waves. In this case, for a bichromatic lattice³, as well as for optical lattice formed by monochromatic light waves, the spatial topology can depend on the relative phase of the waves forming the field^{43,44}. Therefore, the optical lattices with phase-independent topology are of the greatest practical interest. Such lattices can be generally formed by a number of waves M not exceeding $N + 1$, where N is the dimensionality of space. Thus, a 2D configuration of a phase-independent macroscopic optical lattice is formed by a maximum of three

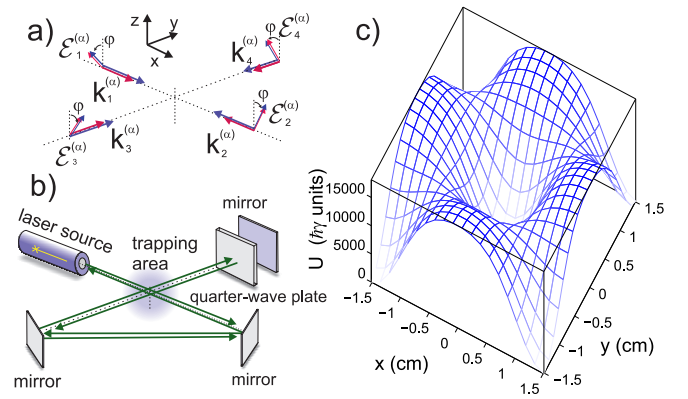


FIG. 7. Macroscopic 2D optical potential formed by four beams of bichromatic light waves with linear polarizations oriented at an angle of $\varphi = \pi/4$ to the z axis (a). The spatial configuration of the field is formed by the geometry of a folded standing wave (b). The macroscopic optical potential (c) has a trapping area depth is $\Delta U \simeq 15200\hbar\gamma \simeq 21$ K. The light field intensity and frequencies of the running waves forming the field corresponds to parameters of Fig.3.

traveling bichromatic waves, and a 3D configuration — by a maximum of four pairs³.

Alternatively, an optical lattice with phase-independent topology can be obtained by combining counter-propagating waves formed by a folded standing wave in both two-dimensional and three-dimensional configurations (Fig.7). In such a field, the phases of the traveling waves are linked, and mirror displacement does not lead to a phase-induced change in the potential shape, but only to its spatial shift⁴⁵. As can be seen (see Fig.7) a 2D configuration with a folded standing wave geometry forms a macroscopic potential in the shape of a well for trapping and cooling atoms. Its depth agrees well with estimates obtained in the one-dimensional model (see Fig. 3). A 3D configuration of a macroscopic optical trap can be formed in a similar manner.

Thus, 2D and 3D optical traps, formed by $lin \perp lin$ configuration in each direction, are an alternative to standard magneto-optical traps for capturing atoms from the hot fraction and for laser cooling atoms to sub-Doppler temperatures.

V. CONCLUSION

In this paper we show that a deep purely optical dissipative macroscopic potential formed by a bichromatic field can be created for alkaline earth and similar atoms. Such a potential can capture and cool atoms directly from the hot fraction, providing an alternative to MOT. Direct numerical calculations were performed using as the example of ^{171}Yb atoms in the field of a double $lin \perp lin$ configuration of counterpropagating waves. In such a field, it is possible to achieve sub-Doppler temperatures $T \simeq 130\mu\text{K}$ (see Fig. 5) of ^{171}Yb trapped atoms, which is unattainable for these atoms in the MOT. In addition, the size of the cold atoms cloud reaches submillimeter values, and the number of atoms is comparable to the number of

atoms in the MOT. The presented purely optical trap can be considered as an alternative to the MOT for quantum sensors, quantum memory and optical frequency standards, which require precise control of the magnetic field in the region of cold atom interrogation.

In conclusion we note, that alkaline-earth and similar atoms possess only a nuclear magnetic moment in the ground state, which is three orders of magnitude smaller than the electronic one. This significantly reduces the sensitivity of proposed laser cooling scheme to residual magnetic fields. Our estimates show that the presence of a residual magnetic field $B < 1$ G does not lead to substantial changes in the presented results. At the same time, such conditions are quite feasible and represent a standard requirement for experimental setups.

ACKNOWLEDGMENTS

The research was supported by grant No. 25-22-00314 from the Russian Science Foundation, <https://rscf.ru/project/25-22-00314/>

DATA AVAILABILITY STATEMENT

Data available on request from the authors

Appendix A

The explicit form of the action of the operators $\hat{\mathcal{L}}^{(k)}$ on a matrix $\hat{\sigma}$ can be written in the form of the equations are given below. The zeroth order $\hat{\mathcal{L}}^{(0)}$ of the expansion in the recoil parameter $-ik_j$ has the form

$$\begin{aligned}\hat{\mathcal{L}}^{(0)}\{\hat{\sigma}\}^{ee} &= -\gamma\hat{\sigma}^{ee} - \frac{i}{\hbar}\left[\hat{H}_0^{ee}\hat{\sigma}^{ee} - \hat{\sigma}^{ee}\hat{H}_0^{ee}\right] \\ &\quad - i\sum_{\alpha=1,2}(\hat{V}_\alpha(\mathbf{r})\hat{\sigma}_\alpha^{ge} - \hat{\sigma}_\alpha^{eg}\hat{V}_\alpha^\dagger(\mathbf{r})), \\ \hat{\mathcal{L}}^{(0)}\{\hat{\sigma}\}^{gg} &= \gamma\sum_{s=0,\pm 1}\hat{D}_s^\dagger\hat{\sigma}^{ee}\hat{D}_s - \frac{i}{\hbar}\left[\hat{H}_0^{gg}\hat{\sigma}^{gg} - \hat{\sigma}^{gg}\hat{H}_0^{gg}\right] \\ &\quad - i\sum_{\alpha=1,2}(\hat{V}_\alpha^\dagger(\mathbf{r})\hat{\sigma}_\alpha^{eg} - \hat{\sigma}_\alpha^{ge}\hat{V}_\alpha(\mathbf{r})), \quad (\text{A.1}) \\ \hat{\mathcal{L}}^{(0)}\{\hat{\sigma}\}_\alpha^{eg} &= -(\gamma/2 - i\omega_\alpha)\hat{\sigma}_\alpha^{eg} - \frac{i}{\hbar}\left[\hat{H}_0^{ee}\hat{\sigma}^{eg} - \hat{\sigma}^{eg}\hat{H}_0^{gg}\right] \\ &\quad - i(\hat{V}_\alpha(\mathbf{r})\hat{\sigma}^{gg} - \hat{\sigma}^{ee}\hat{V}_\alpha(\mathbf{r})), \quad \alpha = 1, 2, \\ \hat{\mathcal{L}}^{(0)}\{\hat{\sigma}\}_\alpha^{ge} &= -(\gamma/2 + i\omega_\alpha)\hat{\sigma}_\alpha^{ge} - \frac{i}{\hbar}\left[\hat{H}_0^{gg}\hat{\sigma}^{ge} - \hat{\sigma}^{ge}\hat{H}_0^{ee}\right] \\ &\quad - i(\hat{V}_\alpha^\dagger(\mathbf{r})\hat{\sigma}^{ee} - \hat{\sigma}^{gg}\hat{V}_\alpha^\dagger(\mathbf{r})), \quad \alpha = 1, 2.\end{aligned}$$

For the j -th Cartesian component of the operator $\hat{\mathcal{L}}^{(1)}$ we

have

$$\begin{aligned}\hat{\mathcal{L}}_j^{(1)}\{\hat{\sigma}\}^{ee} &= -\frac{1}{2}\sum_{\alpha=1,2}(\hat{F}_{\alpha j}\hat{\sigma}_\alpha^{ge} + \hat{\sigma}_\alpha^{eg}\hat{F}_{\alpha j}^\dagger), \\ \hat{\mathcal{L}}_j^{(1)}\{\hat{\sigma}\}^{gg} &= -\frac{1}{2}\sum_{\alpha=1,2}(\hat{F}_{\alpha j}^\dagger\hat{\sigma}_\alpha^{eg} + \hat{\sigma}_\alpha^{ge}\hat{F}_{\alpha j}), \\ \hat{\mathcal{L}}_j^{(1)}\{\hat{\sigma}\}_\alpha^{eg} &= -\frac{1}{2}(\hat{F}_{\alpha j}\hat{\sigma}^{gg} + \hat{\sigma}^{ee}\hat{F}_{\alpha j}), \quad \alpha = 1, 2, \\ \hat{\mathcal{L}}_j^{(1)}\{\hat{\sigma}\}_\alpha^{ge} &= -\frac{1}{2}(\hat{F}_{\alpha j}^\dagger\hat{\sigma}^{ee} + \hat{\sigma}^{gg}\hat{F}_{\alpha j}^\dagger), \quad \alpha = 1, 2,\end{aligned}\quad (\text{A.2})$$

where $\hat{F}_{\alpha j} = -\partial_{\mathbf{r}_j}\hat{V}_\alpha(\mathbf{r})$ is the j -th component of the force operator.

The second order terms are

$$\begin{aligned}\hat{\mathcal{L}}_{jj'}^{(2)}\{\hat{\sigma}\}^{ee} &= \frac{i}{8}\sum_{\alpha=1,2}[(\partial_{\mathbf{r}_j}\partial_{\mathbf{r}_{j'}}\hat{V}_\alpha)\hat{\sigma}_\alpha^{ge} - \hat{\sigma}_\alpha^{eg}(\partial_{\mathbf{r}_j}\partial_{\mathbf{r}_{j'}}\hat{V}_\alpha^\dagger)], \\ \hat{\mathcal{L}}_{jj'}^{(2)}\{\hat{\sigma}\}^{gg} &= \frac{i}{8}\sum_{\alpha=1,2}[(\partial_{\mathbf{r}_j}\partial_{\mathbf{r}_{j'}}\hat{V}_\alpha^\dagger)\hat{\sigma}_\alpha^{eg} - \hat{\sigma}_\alpha^{ge}(\partial_{\mathbf{r}_j}\partial_{\mathbf{r}_{j'}}\hat{V}_\alpha)] \\ &\quad + \hat{\Gamma}_{jj'}^{(2)}\{\hat{\sigma}^{ee}\}, \quad (\text{A.3}) \\ \hat{\mathcal{L}}_{jj'}^{(2)}\{\hat{\sigma}\}_\alpha^{eg} &= \frac{i}{8}[(\partial_{\mathbf{r}_j}\partial_{\mathbf{r}_{j'}}\hat{V}_\alpha)\hat{\sigma}^{gg} - \hat{\sigma}^{ee}(\partial_{\mathbf{r}_j}\partial_{\mathbf{r}_{j'}}\hat{V}_\alpha)], \\ \hat{\mathcal{L}}_{jj'}^{(2)}\{\hat{\sigma}\}_\alpha^{ge} &= \frac{i}{8}[(\partial_{\mathbf{r}_j}\partial_{\mathbf{r}_{j'}}\hat{V}_\alpha^\dagger)\hat{\sigma}^{ee} - \hat{\sigma}^{gg}(\partial_{\mathbf{r}_j}\partial_{\mathbf{r}_{j'}}\hat{V}_\alpha^\dagger)], \\ &\quad \alpha = 1, 2,\end{aligned}$$

which contain contributions proportional to the second derivative of the dipole interaction operators \hat{V}_α . Here $\hat{\Gamma}_{jj'}^{(2)}\{\hat{\sigma}\}$ is the second order of the expansion of the spontaneous relaxation operator (7) in the recoil parameter

$$\hat{\Gamma}_{ij}^{(2)}\{\hat{\sigma}\} = \frac{\gamma}{5}\sum_{m,n}(\delta_{ij}\delta_{mn} - \frac{1}{4}[\delta_{in}\delta_{jm} + \delta_{im}\delta_{jn}])\hat{D}_m^\dagger\hat{\sigma}\hat{D}_n. \quad (\text{A.4})$$

The presented operators $\hat{\mathcal{L}}^{(\kappa)}$, ($\kappa = 0, 1, 2$) allow us to obtain expressions for the force and diffusion tensors on atom in a bichromatic field and to analyze the kinetics of atoms within the framework of the semiclassical Fokker-Planck equation (11).

¹A. Kazantsev, G. Surdutovich, and V. Yakovlev, *Mechanical Action of Light on Atoms* (World Scientific, Singapore, 1990).

²E. Raab, M. Prentis, A. Cable, S. Chu, and D. Pritchard, "Trapping of neutral sodium atoms with radiation pressure," *Phys. Rev. Lett.* **59**, 2631–2634 (1987).

³O. N. Prudnikov, R. Y. Ilenkov, A. V. Taichenachev, V. I. Yudin, and S. N. Bagaev, "Deep macroscopic pure-optical potential for laser cooling and trapping of neutral atoms," *Phys. Rev. A* **108**, 043107 (2023).

⁴A. P. Kazantsev and I. V. Krasnov, "Rectification of the gradient force of resonant radiation pressure," *JETP Lett.* **46**, 332–336 (1987).

⁵R. Grimm, Y. B. Ovchinnikov, A. I. Sidorov, and V. S. Letokhov, "Observation of a strong rectified dipole force in a bichromatic standing light wave," *Phys. Rev. Lett.* **65**, 1415 (1990).

⁶J. Söding, R. Grimm, Y. B. Ovchinnikov, P. Bouyer, and C. Salomon, "Short-distance atomic beam deceleration with a stimulated light force," *Phys. Rev. Lett.* **78**, 1420–1423 (1997).

⁷M. A. Chieda and E. E. Eyler, "Bichromatic slowing of metastable helium," *Phys. Rev. A* **86**, 053415 (2012).

- ⁸T. Na Narong, T. Liu, N. Raghuram, and L. Hollberg, “Stimulated slowing of yb atoms on the narrow $^1S_0 \rightarrow ^3P_1$ transition,” *Phys. Rev. A* **104**, 053117 (2021).
- ⁹O. N. Prudnikov, A. S. Baklanov, A. V. Taichenachev, A. M. Tumaikin, and V. I. Yudin, “Kinetics of atoms in a bichromatic field,” *JETP* **117**, 222–231 (2013).
- ¹⁰O. N. Prudnikov, A. V. Taichenachev, and V. I. Yudin, “Kinetics of atoms in a bichromatic field formed by elliptically polarised waves,” *Quantum Electronics* **47**, 438–445 (2017).
- ¹¹S. Falke, H. Schnatz, J. S. R. V. Winfred, T. Middelmann, S. Vogt, S. Weyers, B. Lipphardt, G. Grosche, F. Riehle, U. Sterr, and C. Lisdat, “The 87sr optical frequency standard at ptb,” *Metrologia* **48**, 399 (2011).
- ¹²N. Poli, C. W. Oates, P. Gill, and G. M. Tino, “Optical atomic clocks,” *La Rivista del Nuovo Cimento* **36**, 555 (2013).
- ¹³A. D. Ludlow, M. M. Boyd, J. Ye, E. Peik, and P. O. Schmidt, “Optical atomic clocks,” *Rev. Mod. Phys.* **87**, 637–701 (2015).
- ¹⁴A. P. Kulosa, D. Fim, K. H. Zippel, S. Rühmann, S. Sauer, N. Jha, K. Gibble, W. Ertmer, E. M. Rasel, M. S. Safronova, U. I. Safronova, and S. G. Porsev, “Towards a mg lattice clock: Observation of the $^1S_0 - ^3P_0$ transition and determination of the magic wavelength,” *Phys. Rev. Lett.* **115**, 240801 (2015).
- ¹⁵A. N. Goncharov, A. E. Bonert, V. I. Baraulya, M. A. Tropnikov, S. A. Kuznetsov, A. V. Taichenachev, and S. N. Bagayev, “Optical atomic clocks,” *Quantum Electronics* **48**, 410 (2018).
- ¹⁶M. Takamoto, I. Ushijima, N. Ohmae, T. Yahagi, K. Kokado, H. Shinkai, and H. Katori, “Test of general relativity by a pair of transportable optical lattice clocks,” *Nat. Photonics* **14**, 411–415 (2020).
- ¹⁷J. P. Covey, A. Sipahigil, S. Szoke, N. Sinclair, M. Endres, and O. Painter, “Telecom-band quantum optics with ytterbium atoms and silicon nanophotonics,” *Phys. Rev. Appl.* **11**, 034044 (2019).
- ¹⁸A. V. Taichenachev, A. N. Goncharov, A. E. Bonert, V. I. Baraulya, M. A. Tropnikov, S. A. Kuznetsov, O. N. Prudnikov, and S. N. Bagaev, “Atom interferometry with ultracold mg atoms: frequency standard and quantum sensors,” *J. Phys.: Conf. Ser.* **1508**, 012002 (2020).
- ¹⁹F. Riehle, A. Witte, T. Kisters, and J. Helmcke, “Interferometry with ca atoms,” *Appl. Phys. B* **54**, 333 (1992).
- ²⁰J. Rudolph, T. Wilkason, M. Nantel, H. Swan, C. M. Holland, Y. Jiang, B. E. Garber, S. P. Carman, and J. M. Hogan, “Large momentum transfer clock atom interferometry on the 689 nm intercombination line of strontium,” *Phys. Rev. Lett.* **124**, 083604 (2020).
- ²¹L. Hu, E. Wang, L. Salvi, J. N. Tinsley, G. M. Tino, and N. Poli, “Sr atom interferometry with the optical clock transition as a gravimeter and a gravity gradiometer,” *Classical and Quantum Gravity* **37**, 014001 (2019).
- ²²C. Adams and E. Riis, “Laser cooling and trapping of neutral atoms,” *Prog. Quonr. Electr* **21**, 1 (1997).
- ²³A. Bizzarri and M. C. E. Huber, “Transition probabilities from the $6s6p\ ^1P^{\circ}_1$ resonance level of neutral barium,” *Phys. Rev. A* **42**, 5422–5424 (1990).
- ²⁴J. Brust and A. C. Gallagher, “Excitation transfer in barium by collisions with noble gases,” *Phys. Rev. A* **52**, 2120–2131 (1995).
- ²⁵M. Kleinert, M. E. Gold Dahl, and S. Bergeson, “Measurement of the yb i $^1S_0 - ^1P_1$ transition frequency at 399 nm using an optical frequency comb,” *Phys. Rev. A* **94**, 052511 (2016).
- ²⁶R. Maruyama, R. H. Wynar, M. V. Romalis, A. Andalkar, M. D. Swallows, C. E. Pearson, and E. N. Fortson, “Investigation of sub-doppler cooling in an ytterbium magneto-optical trap,” *Phys. Rev. A* **68**, 011403 (2003).
- ²⁷H. Katori, T. Ido, Y. Isoya, and M. Kuwata-Gonokami, “Magneto-optical trapping and cooling of strontium atoms down to the photon recoil temperature,” *Phys. Rev. Lett.* **82**, 1116–1119 (1999).
- ²⁸O. N. Prudnikov, R. Y. Il’enkov, A. V. Taichenachev, and V. I. Yudin, “Scaling law in laser cooling on narrow-line optical transitions,” *Phys. Rev. A* **99**, 023427 (2019).
- ²⁹O. N. Prudnikov, R. Y. Ilenkov, A. V. Taichenachev, A. M. Tumaikin, and V. I. Yudin, “Steady state of a low-density ensemble of atoms in a monochromatic field taking into account recoil effects,” *JETP* **112**, 939–945 (2011).
- ³⁰J. Dalibard and C. Cohen-Tannoudji, “Atomic motion in laser light: connection between semiclassical and quantum descriptions,” *J.Phys. B.* **18**, 1661–1683 (1985).
- ³¹J. Javanainen, “Density-matrix equations and photon recoil for multistate atoms,” *Phys. Rev. A* **44**, 5857–5880 (1991).
- ³²S. M. Yoo and J. Javanainen, “Low-intensity limit of the laser cooling of a multistate atom,” *Phys. Rev. A* **45**, 3071–3083 (1992).
- ³³O. N. Prudnikov, A. V. Taichenachev, A. M. Tumaikin, and V. I. Yudin, “Polarization-gradient laser cooling as a way to create strongly localized structures for atom lithography,” *Phys. Rev. A* **75**, 023413 (2007).
- ³⁴A. A. Kirpichnikova, O. N. Prudnikov, R. Y. Il’enkov, A. V. Taichenachev, and V. I. Yudin, “Laser cooling limits in fields with a polarisation gradient of atoms with different recoil energies,” *Quantum Electronics* **50**, 939–946 (2020).
- ³⁵A. A. Kirpichnikova, O. N. Prudnikov, A. V. Taichenachev, and V. I. Yudin, “Itô – stratonovich dilemma in the problem of laser cooling of atoms: limits of applicability of the semiclassical approximation,” *Quantum Electronics* **52**, 130 – 136 (2022).
- ³⁶A. V. Bezvernyi, O. N. Prudnikov, A. V. Taichenachev, A. V. Tumaikin, and V. I. Yudin, “The light pressure force and the friction and diffusion coefficients for atoms in a resonant nonuniformly polarized laser field,” *JETP* **96**, 383–401 (2003).
- ³⁷O. N. Prudnikov, A. V. Taichenachev, A. V. Tumaikin, and V. I. Yudin, “Kinetics of atoms in the field produced by elliptically polarized waves,” *JETP* **98**, 438–454 (2004).
- ³⁸J. Dalibard and C. Cohen-Tannoudji, “Laser cooling below the doppler limit by polarization gradients: simple theoretical models,” *J. Opt. Soc. Am. B* **6**, 2023–2045 (1989).
- ³⁹C. Monroe, W. Swann, H. Robinson, and C. Wieman, “Very cold trapped atoms in a vapor cell,” *Phys. Rev. Lett.* **65**, 1571–1574 (1990).
- ⁴⁰K. E. Gibble, S. Kasapi, and S. Chu, “Improved magneto-optic trapping in a vapor cell,” *Opt. Lett.* **17**, 526–528 (1992).
- ⁴¹J. Javanainen, “Numerical experiments in semiclassical laser-cooling theory of multistate atoms,” *Phys. Rev. A* **46**, 5819–5835 (1992).
- ⁴²O. N. Prudnikov and E. Arimondo, “Quasiclassical laser cooling in an intense standing wave,” *J. Opt. B: Quantum Semiclass. Opt.* **6**, 336–344 (2004).
- ⁴³P. Jessen and I. Deutsch, “Optical lattices,” *Advances In Atomic, Molecular, and Optical Physics* **37**, 95–138 (1996).
- ⁴⁴A. Hemmerich and T. W. Hänsch, “Two-dimensional atomic crystal bound by light,” *Phys. Rev. Lett.* **70**, 410–413 (1993).
- ⁴⁵G. D. Domenico, N. Castagna, P. M.D., T. P., T. A.V., and Y. V.I., “On the stability of optical lattices,” *Laser Physics* **15**, 1674–1679 (2005).